ISSN 1069-3513, Izvestiya, Physics of the Solid Earth, 2013, Vol. 49, No. 5, pp. 675–682. © Pleiades Publishing, Ltd., 2013.
Original Russian Text © M.Yu. Reshetnyak, 2013, published in Fizika Zemli, 2013, No. 5, pp. 81–88.

Convection in Anelastic Models of the Earth's Liquid Core

M. Yu. Reshetnyak

Schmidt Institute of Physics of the Earth, Russian Academy of Sciences, ul. Bol'shaya Gruzinskaya 10, Moscow, 123995 Russia

Received January 31, 2013

Abstract—The effects of adiabatic cooling on the convection in the anelastic model of the liquid core of the Earth are considered. It is shown that even minor adiabatic cooling causes significant changes in the pattern of the convection, shifting the peak in the convection intensity to the inner part of the core. Just as in the Boussinesq model, both direct and inverse kinetic energy cascades are simultaneously present, and the direct cascade of entropy is observed.

Keywords: geodynamo, cascade phenomena, adiabatic cooling, entropy

DOI: 10.1134/S1069351313050054

INTRODUCTION

Convection in the cores of planets is a source of energy for the observed planetary magnetic fields. According to the modern theories, fast rotating cores of planets maintain geostrophic balance with the pressure gradient equilibrated by the Coriolis force (Pedlosky, 1987). As it follows from the linear analysis, at the excitation threshold of the convection with fast rotation, the ratio of the horizontal scale of the flow to the scale along the rotational axis is $l_c \sim E^{1/3}$ (Busse, 1970), where Ekman's number for Earth $E \approx 10^{-15}$ is very small. Such a low ratio of viscous forces to the forces of rotation, which is determined by E, results in the strong anisotropy of the flows (Hejda and Reshetnyak, 2009). Although the intensity of the heat sources in the core is by a few orders of magnitude higher than critical, the degree of anisotropy is still very high.

In spectral space, rotation leads to the emergence of local maxima in the spectra of kinetic energy and temperature fluctuations, which correspond to the scale l_c. At the excitation threshold, this spectral maximum is global. As the intensity of thermal sources further increases, an additional large-scale component arises, and the maximum at l_c becomes local. Moreover, in the interval of l_c up to L, where L is the scale size of the liquid core, the spectrum becomes filled; however, the kinetic energy is transferred in the opposite direction (from l_c to L). Recall that in the case of a common three-dimensional (3D) convection without rotation, the conventional direct energy cascade from large scales to small scales is observed. The inverse energy cascade in geostrophic turbulence was observed in the models with both the plane geometry (Reshetnyak and Hejda, 2008) and spherical geometry (Reshetnyak and Hejda, 2012). In other words, in addition to the well known α-effect (Krause and Rädler, 1980), which leads to the generation of the large-scale planetary (dipole) magnetic field due to the turbulent energy, also another synergetic (purely hydrodynamic) effect is possible, when the large-scale flows gain energy from turbulence. This effect is well known in two-dimensional (2D) turbulence (Lesieur, 1990) and is due to the conservation of entropy.

Generally speaking, the existence of inverse cascades is associated with a fundamental difficulty, which stems from the necessity to take off the energy supplied to the large scales, where dissipation is low. In contrast to the simplest cascade turbulence models (Frick, 2010) where it was possible to artificially render the energy takeoff from the large scales by the mechanism of Rayleigh friction, in the self-consistent three-dimensional (3D) models, the energy cascades of both directions can exist along the rotational **z** axis and in the perpendicular plane to **z**. Moreover, not only the transfer of kinetic energy but also the thermal energy transfer throughout the spectrum should be taken into account. The comparison between the flows of thermal and kinetic energy is important also from the standpoint that the rotation leads to the weakening of the kinetic energy cascade, and the contribution of the latter could be small compared to the flow of the total energy (thermal and kinetic).

Since all the quoted papers on the detection of the inverse cascades of kinetic energy were based on the Boussinesq approximation, which cannot adequately allow for the thermal energy, we then analyze the anelastic model, which takes into account the compressibility of the medium. This model for the liquid core of the Earth has been first considered in detail in (Braginsky and Roberts, 1995) and then used for 3D calculations in (Glatzmaier and Roberts, 1996). Besides the fact that it allows for compressibility, this model also differs from the Boussinesq model by the

presence of negative energy sources in the right-hand side of the heat transfer equation—the so-called adiabatic cooling, whose implications for the properties of the convection will also be analyzed below in the 3D numerical anelastic convection model.

THE PHYSICAL MODEL

The main idea of the anelastic model is that the acoustic waves in the convection equations for the compressible viscous medium are ignored (see (Braginsky and Roberts, 1995; Jones, 2007) for more detail). It is then assumed that the average density $\bar{\rho}$ in a spherical shell ($r_{ICB} \le r \le r_{CMB}$)[1] only depends on radius r, which gives the following form of the continuity equation: $\nabla \cdot (\bar{\rho}\mathbf{V}) = 0$, where $\mathbf{V}$ is the velocity field and (r, θ, φ) are spherical coordinates.

The thermal convection in the spherical shell that is rotating about axis $\mathbf{z}$ with angular velocity Ω is described by the dimensionless Navier-Stokes equation and the equation for entropy S:

$$\begin{aligned}
\mathrm{Pr}^{-1}\mathrm{E}\bar{\rho}\frac{\partial \mathbf{V}}{\partial t} &= -\mathrm{Pr}^{-1}\mathrm{E}\nabla\cdot(\bar{\rho}\mathbf{V}\otimes\mathbf{V}) - \nabla P - \bar{\rho}\mathbf{1}_z\mathbf{V} \\
&- \mathrm{R}\bar{\rho}\frac{d\bar{T}}{dr}S\mathbf{1}_r + \mathrm{E}\bar{\rho}\nabla^2\mathbf{V} + \frac{\mathrm{E}}{3}\bar{\rho}\nabla(\nabla\cdot\mathbf{V}), \\
\bar{\rho}\frac{\partial S}{\partial t} &+ \bar{\rho}(\nabla\cdot\mathbf{V})S \\
&= \bar{\rho}\nabla^2 S + \frac{1}{\bar{T}}\frac{d\bar{T}\bar{\rho}}{dr}\frac{dS}{dr} + \frac{Q}{\bar{T}r^2}\frac{d}{dr}\left(r^2\bar{\rho}\frac{d\bar{T}}{dr}\right).
\end{aligned} \tag{1}$$

In Eq. (1), the length is measured in the units of the radius of liquid core L, so that $r_{CMB} = 1$ and the radius of the solid core r_{ICB} is 0.35. The velocity $\mathbf{V}$, total pressure P, and characteristic diffusion time t are measured in units of k^S/L, $\rho(k^S/\mathrm{L})^2$, and L^2/k^S, respectively. Here, k^S is the turbulent diffusion coefficient for S; $\mathrm{Pr} = \frac{\nu}{k^S}$ and $\mathrm{E} = \frac{\nu}{2\Omega\mathrm{L}^2}$ are the dimensionless Prandtl and Ekman numbers; and ν is kinematic viscosity. For the adiabatic state, which is assumed for the liquid core of the Earth, by analogy to (Glatzmaier and Roberts, 1996), we use the normalized profiles for average density $\bar{\rho} = 1.148 - 0.237r^2$ and adiabatic temperature $\bar{T} = \bar{\rho}_\gamma$, where $\gamma = 1.35$ is the Grüneisen parameter.

The intensity of the heat sources is specified by the quantity $\mathrm{R} = \frac{\delta S \delta T}{\Omega k^S}$, where $\delta T = T_{ICB} - T_{CMB}$, and δS is the characteristic amplitude of variations in entropy. Upon diffusive nondimensionalization, R does not include scale L, although for the modified Rayleigh number (Jones, 2000) $\mathrm{Ra} = \frac{\alpha g_0 \delta T \mathrm{L}}{2\Omega k}$, this dependence on ~L exists. This is associated with the fact that for the coefficient of volumetric thermal expansion $\alpha = -\frac{C_p}{g}\frac{1}{\bar{T}}\frac{d\bar{T}}{dr}$, where C_p is specific heat capacity at constant pressure and g is gravitational acceleration, we have $\alpha \sim \frac{C_p}{g\mathrm{L}}$, which in the case of large jumps in temperature gives the desired dependence on L in Ra. Until the further discussion of the relationship between δT and δS, we assume that these measurement units for $\bar{T}$ and S are independent.

The last parameter Q is the measure of adiabatic cooling $Q = \frac{C_p k^T}{\delta S k^S}$, where k^T is the coefficient of thermal diffusion. In contrast to (Glatzmaier and Roberts, 1996), the buoyancy force $\mathrm{R}\bar{\rho}\frac{d\bar{T}}{dr}S\mathbf{1}_r$ in the Navier-Stokes equation is here only proportional to the fluctuations in entropy S but independent of the fluctuations in pressure (Braginsky and Roberts, 1995; Anufriev, Jones, and Soward, 2005).

Since we do not further consider the details associated with the growth of the solid core, the equation for the admixture is also not considered, and we may use the simplified boundary equations for S: $S_{ICB} = 1$, $S_{CMB} = 0$ (Jones et al., 2011) and no-slip and no-penetration conditions for $\mathbf{V}$.

Equations (1) are solved using the MPI-code (Reshetnyak, 2012) tailored for the compressible medium. This code relies on standard decompositions in spherical functions and Chebyshev polynomials, as well as on the decomposition of the solenoidal field $\bar{\rho}\mathbf{V}$ into its poloidal and toroidal components; after this, the curl and double curl operators are applied to the Navier-Stokes equation in order to eliminate pressure.

THE RADIAL PROFILES AND TIME EVOLUTION

Although the first numerical 3D anelastic geodynamo model (Glatzmaier and Roberts, 1996) has been developed as early as one year after the Boussinesq model (Glatzmaier and Roberts, 1995), this model has long remained the single example that uses the full thermodynamic equations (Braginsky and Roberts, 1995). One reason was purely technical and associated with the introduction of the additional equation for pressure, which has been excluded in the previous models.

[1] ICB stands for the boundary between the liquid core and solid core; CMB stands for the core-mantle boundary.

Besides, in the first models, all the equations were solved simultaneously, which produced a very large matrix during the solution of the system of linear equations and, correspondingly, resulted in a high computational burden. Later, equations were solved in successive order, and since than, the additional Poisson equation for P has no longer increased the volume of computations noticeably.

Another reason to prefer the Boussinesq model, which is simpler, was the weak effect of the compressibility of liquid iron on the core of the Earth. Since even today the accuracy of a number of the quantities, including the rate of planetary rotation and viscous effects, still differs by orders of magnitude from the required geophysical values, ignoring a 20% jump in density along the thickness of the liquid core was not considered to be too misleading (Fig. 1a).

The next distinction arising in the anelastic model is related to the assumption of adiabatic liquid core. For example, the Boussinesq model uses two types of boundary conditions: either the temperatures or the heat flows are specified on the solid boundaries with the heat sources present in the bulk of the core. These boundary conditions correspond to the hyperbolic or parabolic temperature profile in the absence of the convection. In contrast to this, in the anelastic model, the shape of the conductive temperature profile was specified by the adiabat $\bar{T}$.

The entropy equation in (1) differs from the equation for temperature in the Boussinesq approximation by two terms in the right-hand side: $f_1\frac{dS}{dr}$, where $f_1 = \frac{1}{\bar{T}}\frac{d\bar{T}\bar{\rho}}{dr}$, and $f_2 = \frac{1}{\bar{T}r^2}\frac{d}{dr}\left(r^2\bar{\rho}\frac{d\bar{T}}{dr}\right)$. To ensure that we interpret the solution of nonlinear problem (1) correctly, we explore how these two terms affect the solution of a simple spherically symmetric stationary problem for the equation for S in the absence of convection:

$$\bar{\rho}\frac{1}{r^2}\frac{\partial}{\partial r}\left(r^2\frac{\partial}{\partial r}S\right) + f_1\frac{dS}{dr} + f_2 = 0 \qquad (2)$$

with fixed $(C, 0)$ for $S(r)$ on the boundaries r_{ICB} and r_{CMB}, where C is a positive constant (Figs. 1b–1d).

With $C = 1$, the deviation of both solutions with nonzero f_1 and f_2 from the hyperbolic profile with $f_1 = 0$ and $f_2 = 0$ are negligibly small. Moreover, the first term f_1 for all the considered C gives a flatter profile $S(r)$. The second term f_2 (adiabatic cooling), which introduces inhomogeneity in Eq. (2), causes significant changes in $S(r)$ at higher C and produces negative values of S (Figs. 1c and 1d). The negative S give negative buoyancy force $\sim -\frac{d\bar{T}}{dr}S$, directed towards the center of the Earth, which suppresses the convection by generating the state of stable equilibrium in the outer part of the core. Below it will be shown that in the presence of convection, even the regime with $C = 1$ significantly differs from the Boussinesq

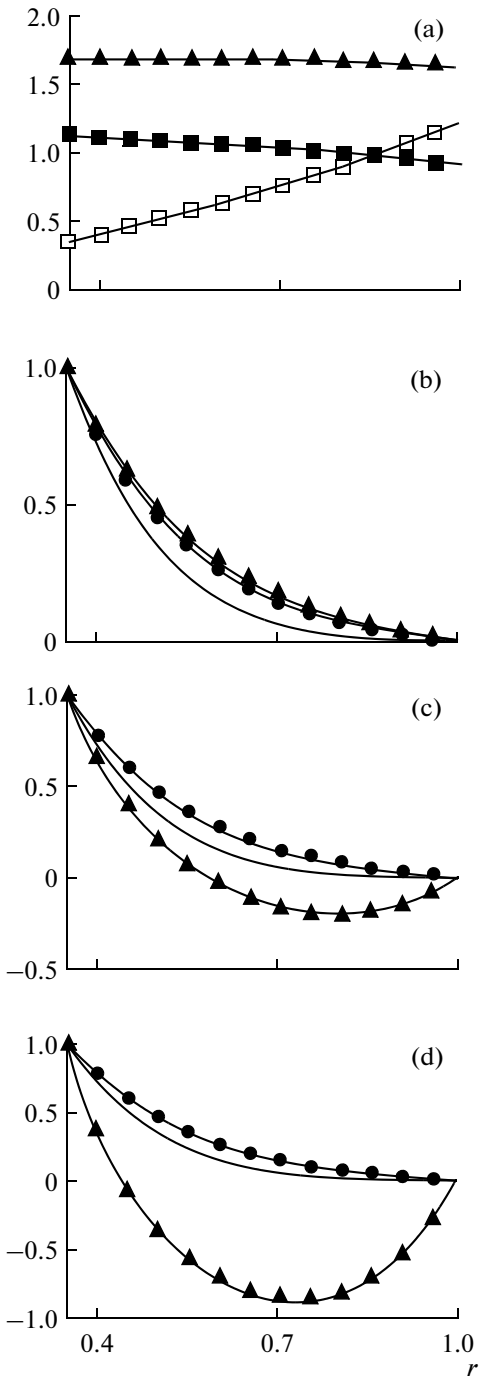

Fig. 1. (a) The radial profiles of $\bar{\rho}$ (the black squares); $-f_1/\bar{\rho}$ (the white squares); $-f_2/\bar{\rho}$ (the triangles); the solution S/C of Eq. (2) for three regimes: (b) $C = 1$; (c) $C = 0.1$; (d) $C = 0.035$. The solid line corresponds to $f_1 = f_2 = 0$; the circles, to $f_2 = 0$, and the triangles, to the regimes f_1, f_2.

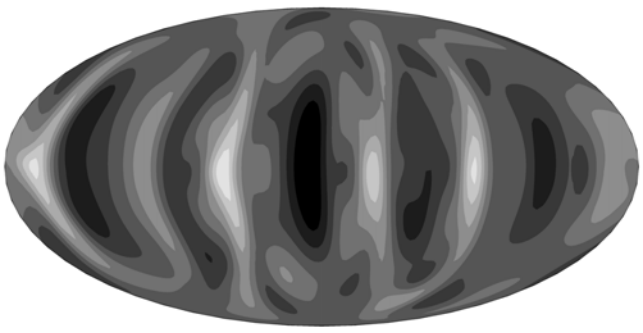

Fig. 2. The Mollweide projection of the $\mathbf{V_r}$ velocity component for R = 6500, E = 2×10^{-4} and Pr = 1 for $r = 0.5$. The field ranges from −120 to 167.

solution at sufficiently large R. We note that adiabatic cooling is an analog of the radioactive heat sources, which were often used previously in the Boussinesq models, but here these sources are taken with a negative sign (Fig. 1a). Thus, the volumetric cooling of the core results in the enhancement of the convection near the lower boundary of the liquid core and in its suppression near the upper boundary.

In order to estimate δS and Q, we cast the three terms in the right-hand side of the equation for S in Eq. (1) in dimensional form:

$$\rho k^S \nabla^2 S + \frac{1}{T}\frac{dT\rho k^S}{dr}\frac{dS}{dr} + \frac{1}{Tr^2}\frac{d}{dr}\left(r^2 \rho C_P k^T \frac{dT}{dr}\right). \qquad (3)$$

Let C_P = 840 J kg^{-1}K^{-1}, k^S = 2 m^2 s^{-1}, and let $k^T = 10^{-5}$ m^2 s^{-1} be specified by $k^T = C_7 \frac{T}{C_P \rho \eta}$, C_7 = 0.02 kg m^3 K^{-2} s^{-4} according to (Glatzmaier and Roberts, 1996). If we assume that the second term is larger than the third term, then $\delta S/l_s \sim 10^{-2}\, k^T/k^S C_P$, where l_s is the characteristic amplitude of fluctuations in S, which, with $l_s = 0.1$L gives $\delta S < 4 \times 10^{-4}$ J kg^{-1} K^{-1}. With this estimate for δS, we obtain R = 3×10^4, where $\Omega = 7 \times 10^{-5}$ s^{-1}, and $Q \approx 1$.

In order to suppress the cyclonic convection on the l_c scales, we used the turbulent viscosity ν^T = 2.8 × 10^4 m^2 s^{-1}, which is commensurate with the value 1.45×10^3 m^2 s^{-1} in (Glatzmaier and Roberts, 1996), where the authors used the hyperviscosity. The turbulent Ekman number in our model was E = 2×10^{-4}. The typical distribution of the emerging cyclones is shown in Fig. 2. The estimation of the typical velocity gives $V \sim 100\, k^S/\mathrm{L} = 2 \times 10^{-4}$ m s^{-1}, which is close to the velocity of the westward drift $V_{\mathrm{wd}} = 6 \times 10^{-5}$ m s^{-1}.

Prior to passing to the analysis of the last term in Eq. (3), we estimate the ratio between the convective $\sim \frac{V^3}{l}$ and thermal $\sim \frac{T\bar{\rho} VS'}{l}$, energy fluxes, where $T = \bar{T} + T'$, $S = \bar{S} + S'$, and $T' = \bar{T}S'/C_P$ (Anufriev, Jones, and Soward, 2005); l is the turbulent scale; and ' means the fluctuating component of the field.

Then, for the solution in (Glatzmaier and Roberts, 1996), we have $\mathcal{R}^{K/S} = \bar{\rho}\frac{V^3}{l} : \bar{\rho}\frac{\bar{T}VS'}{l} = V^2 : \bar{T}S'$. With $\bar{T} = 5 \times 10^3$ K, $V = 6 \times 10^{-4}$ m s^{-1}, and $S' = 10^{-4}$ J kg^{-1} K^{-1}, we come to $\mathcal{R}^{K/S} = 7 \times 10^{-7}$. This estimate, based on the flux $(S')^2$, gives $\mathcal{R}^{K/S^2} = \bar{\rho}\frac{V^3}{l} : \bar{\rho}\frac{T'VS'}{l} = V^2 C_P : \bar{T}(S')^2 \approx 6$.

In our calculations, the estimate, within the order of magnitude of the ratio, is $\mathcal{R}^{K/S} = V^2\left(\frac{k^S}{\mathrm{L}}\right) : TS'\delta S \approx 2 \times 10^{-7}$ and $\mathcal{R}^{K/S^2} \approx 4$. The smallness of $\mathcal{R}^{K/S}$ was the reason to disregard the nonlinear term in the Navier-Stokes equation in the first works on the 3D geodynamo (Glatzmaier and Roberts, 1995), which allowed their authors to reduce the time of the computations without qualitatively changing the final result. However, in the course of the subsequent calculations (Christensen and Aubert, 2006; Schrinner et al., 2010), where hyperviscosity was abandoned, it turned out that the situation is more complex, and the geostrophy of the flows is tightly related to the time behavior of the geomagnetic dipole. It was shown that the violation of geostrophy with the increase in the Rossby number leads to the transition from the rare reversals of the magnetic field dominated by the dipole component to the chaotic flips in the polarity of the magnetic field with a smaller dipole contribution. Our estimate of $\mathcal{R}^{K/S^2}$ also testifies in favor of the larger value of the convective term in the Navier-Stokes equation: the kinetic energy flux is even higher than the thermal energy flux $(S')^2$ ($\mathcal{R}^{K/S^2} > 1$), which just leads to the approach of the nonlinear regime of the arising thermal instability in the equations of thermal convection. This proves that the nonlinear term in the Navier-Stokes equations should not be ignored.

In order to assess the contribution of the two last terms in Eq. (3), we switch them off at the time instant $t = 5.5$ (Fig. 3). Even in the case of $C = 1$, when the variation in the conductive profile $S(r)$ was insignificant (Fig. 1b), the kinetic energy E_K in the convective regime has changed by a factor of 2. The dependence of the kinetic energy on the degree of stratification (which is formally analogous to the action of adiabatic cooling in anelastic models) is a complex phenomenon depending on the particular parameters (Shimkanin, Hejda, and

Saxonbergova-Jankovichova, 2010; Shimkanin, Hejda, and Saxonbergova, 2011). In our case, we observe the reduction of the convection area and the growth in the gradients of S, which results in the increase of the fields of total E_K (Figs. 3 and 4).

The increase in S^2 due to adiabatic cooling in not so trivial, since the larger the Re the thinner the boundary layers the stronger the material inside the main volume is mixed and the smaller the value of S^2 in this volume.

Consider the r-profile of E_K and S (Fig. 5). Remarkably, the adiabatic cooling, which boosts the total kinetic energy in the volume E_K, shifts the peak in E_K towards the lower boundary. This strikingly differs from the case of the Boussinesq convection with fixed temperatures, where the distribution of E_K far from the boundaries does not depend on r. Just as in the case without convection, the contribution of the second term to Eq. (3) is small. It is worth noting that the behavior of $S^2(r)$ is close to the profile in Fig. 1d for much lower values of C. In other words, with this R, the distributions of E_k and S^2 turn out to be more sensitive to the emergence of adiabatic cooling than at R = 0 without convection. This is rather unexpected result, which calls for analyzing the interval of R, where it is observed. A probable explanation is that in the convection regime considered above, the main variations in S occur in the boundary layers, which corresponds to small C in problem (2).

Thus, having considered some features of the convection with adiabatic cooling in the physical medium, we pass to analyzing the spectral properties of the problem.

THE SPECTRA AND THE FLOWS

The cyclonic structure of the geostrophic convection is clearly expressed in the spectra for kinetic energy and entropy. The first exciting mode with $m_c = 3$ is better pronounced in the spectrum of kinetic energy (Fig. 6). Since S also includes the spherically symmetric conductive component, spectrum S contains the axisymmetric mode with $m = 0$. The increase in R results in the filling of the spectrum at $m < m_c$. Adiabatic cooling slightly affects the spectra of E_K and S and only changes the amplitudes of the fields as mentioned before.

Even in the case of quasi steady-state convection, energy can be transferred across the spectrum due to the different locations (in the wave space) of the energy source and dissipation. In contrast to the Kolmogorov's conventional turbulence, where the energy is transferred from large scales to small scales, in the case of rotating turbulence we observe the inverse energy cascade (from l_c to L) (see (Reshetnyak and Hejda, 2008; 2012; Hejda and Reshetnyak, 2009), where the authors used the convection models in the Boussinesq approxi-

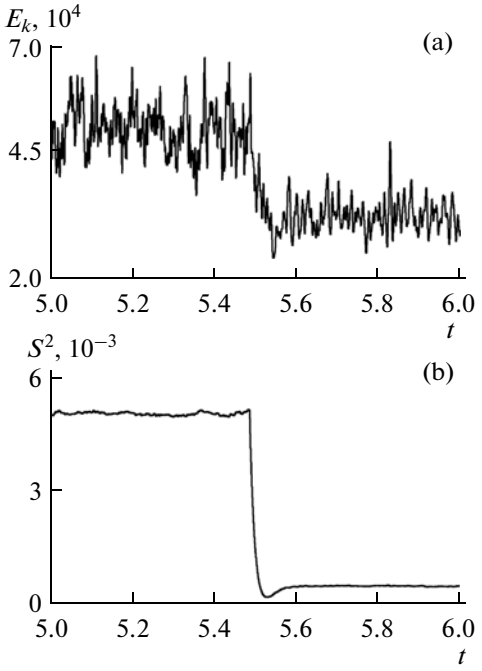

Fig. 3. The evolution of (a) kinetic energy E_k and (b) squared entropy S^2 for $R = 1.8 \times 10^4$ and $E = 2 \times 10^{-4}$. At time $t = 5.5$, two last terms in Eq. (3) are switched off.

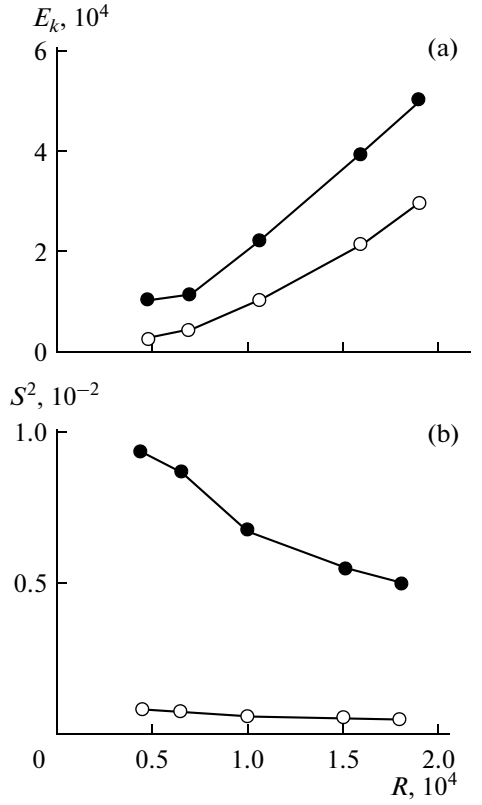

Fig. 4. The dependence of (a) kinetic energy E_k and (b) squared entropy S^2 on the intensity of the heat sources R. The black circles correspond to the solution of Eq. (3) when all the three terms are nonzero; the white circles correspond to the solution with the omitted third term.

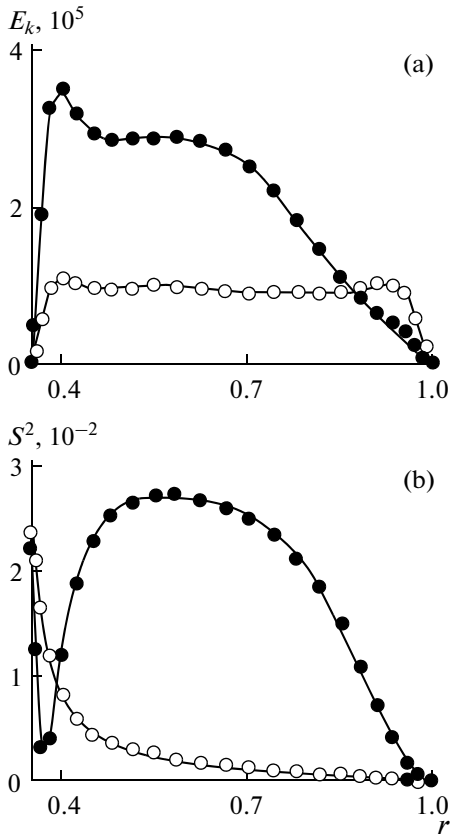

Fig. 5. The radial distribution of (a) kinetic energy E_k and (b) squared entropy S^2 for $R = 1.8 \times 10^4$ and $E = 2 \times 10^{-4}$. The black circles correspond to the solution of Eq. (3) before $t = 5.5$; the white circles correspond to the regime when the both last terms in Eq. (3) are switched off.

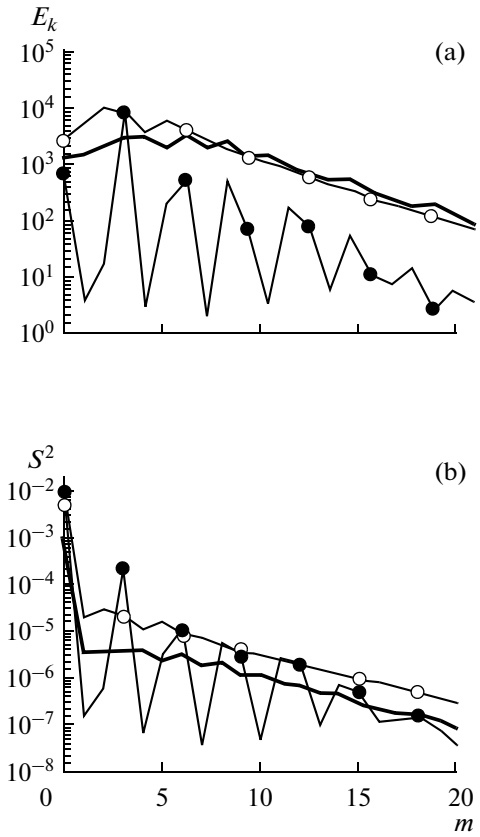

Fig. 6. The spectrum of (1) kinetic energy and (2) entropy for two regimes with $R = 4.5 \times 10^3$(the white circles) and $R = 1.8 \times 10^4$ (the black circles). The thick line corresponds to the second regime, when the both terms in Eq. (3) are switched off.

mation). Let us now consider how this effect manifests itself in the anelastic model, which includes adiabatic cooling. Since the anelastic model is suitable for quantitatively comparing the flows of thermal and kinetic energy, the flows of S will be considered also in the wave space.

Following (Reshtnyak and Hejda, 2012), we introduce the integral flow of the kinetic energy in the wave space, which comes to the sphere $m \le M$ from the modes with $m > M$: $\Pi^K(M) = -\bar{\rho}[(\mathbf{V}\cdot\nabla)\mathbf{V}]\cdot\mathbf{V}^<$, where $\mathbf{V}^<$ denotes the part of the field $\mathbf{V}$ with the filtered harmonics with $m > M$. Since the integral of a nonlinear term over the entire volume in the physical space is zero, then, by Parseval's theorem, $\Pi^K(M)$ also tends to zero at large M.

If $\Pi^K(M) < 0$, the energy is transferred from the large scales to small scales, which corresponds to the direct energy cascade. Positive Π^K corresponds to the direct cascade. As follows from Fig. 7a, the modes with $m < 3$ gain the kinetic energy from the small scales. The adiabatic cooling, which enhances the convection near the solid core and renders it close to Kolmogorov's pattern, slightly weakens this effect.

By analogy to Π^K, we introduce the convective thermal flow $\Pi^S(M) = T\nabla\cdot(\bar{\rho}\mathbf{V}^<S'),$, where $S' = S - \bar{S}$ is the fluctuating convective part of S, which results from the subtraction of the conductive component S from $\bar{S}$, and $T = \bar{T} + T'$ with $T' = \bar{T}S'/C_P$ (Anufriev, Jones, and Soward, 2005). Then, $\hat{\Pi}^S(M) = \bar{T}\left(1 + \frac{S'}{C_P}\right)\nabla\cdot(\bar{\rho}\mathbf{V}^<S') = \bar{T}\nabla\cdot(\bar{\rho}\mathbf{V}^<S') + \Pi^S(M)$, where the term $\Pi^S(M) = \frac{1}{2}\frac{\bar{T}}{C_P}\nabla\cdot(\bar{\rho}\mathbf{V}^<(S')^2)$ has the similar structure as $\Pi^K(M)$ and can be analyzed by the same method. Further, we omit the analysis of the term $\hat{\Pi}^S(M)$, which is associated with the direct cascade of thermal energy from $\bar{T}$.

In contrast to the flow Π^K, the entropy cascade is always direct (Fig. 7b), despite the presence of a local maximum at m_c. The latter is associated with the existence of different integrals of motion in the Navier-Stokes equation and in the heat transfer equation.

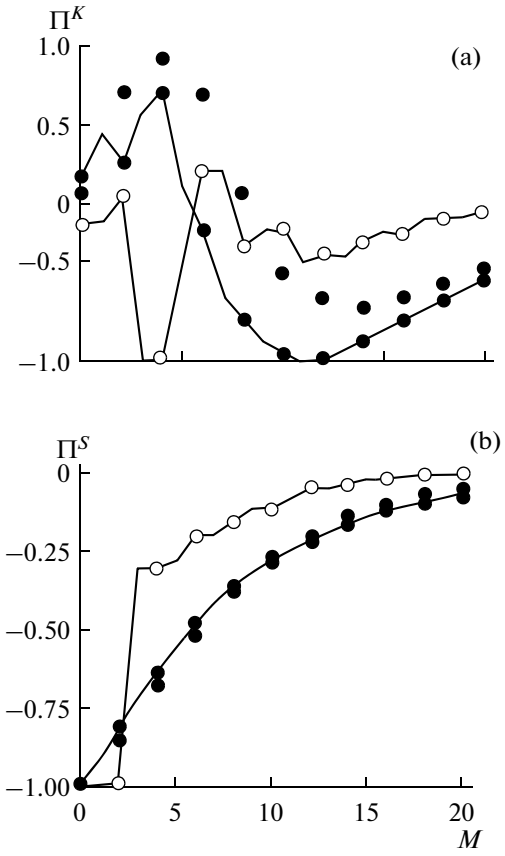

Fig. 7. The normalized fluxes of the (a) kinetic Π^K and thermal Π^S energy for two regimes with $R = 4.5 \times 10^3$ (the white circles) and $R = 1.8 \times 10^4$ (the black circles). For the case (a), the dots connected by the lines correspond to the regime with $R = 1.8 \times 10^4$ with stratification. The dots that are not connected by the lines correspond to the regime with $R = 1.8 \times 10^4$ without stratification. The normalizing coefficients for graph (a) are 4.53, 43.91, and, without stratification—27.43; for graph (b), these are—0.013 and 0.023.

The numerical estimate over the entire volume yields $\mathcal{R}^{K/S} \approx 2 \times 10^{-6}$ and $\mathcal{R}^{K/S^2} \approx 4$, which is close to our previous estimate of $\mathcal{R}^{K/S}$ within the order of magnitude. Such a high value of the inverse convective flow of kinetic energy, which exceeds the thermal flow, is an important feature of thermal convection in the Earth's core.

DISCUSSION

The geodynamo problem is quite specific, since the geomagnetic observations with rather rough spatial resolution but on quite long time intervals should be correlated to the patterns of the model fields, which are calculated with extremely high spatial resolution but on short time intervals (dictated by the computational capabilities). This inconsistency in the spatial resolution is associated with both the specificity of geomagnetic observations and the necessity to ensure geostrophic balance in the models, which results in small $\sim l_c$.

The transition to the simpler model requires knowing the physics of the small-scale processes. An instructive example illustrating this is the application of the apparatus of the mean-field theory, which suggests a straightforward mechanism of energy transfer from turbulence to the large-scale magnetic fields. Above, we have considered how a similar synergetic effect can also arise in the absence of the magnetic field in the models of thermal convection with low Rossby numbers. It turns out that the amplitude of the inverse cascade of kinetic energy is even higher than the turbulent cascade of the thermal energy in the heat transfer equation; i.e., it is quite a strong effect. This approach can be applied in the semiempirical models of turbulent viscosity similar to (Buffet, 2003; Matsushima, 2005).

Another important application of the results is the study of the dynamo regimes, where the magnetic field is concentrated within the internal regions of the liquid core. Since the adiabatic cooling leads to the shift of the peak of kinetic energy towards the solid core, this mechanism can act in the planetary dynamo.

REFERENCES

Anufriev, A.P., Jones, C.A., and Soward, A.M., The Boussinesq and anelastic liquid approximations for convection in the Earth's core, *Phys. Earth Planet. Inter.*, 2005, vol. 152, pp. 163–190.

Braginsky, S.I. and Roberts, P.H., Equations governing convection in Earth's core and the geodynamo, *Geophys. Astrophys. Fluid Dyn.*, 1995, vol. 79, pp. 1–97.

Buffett, B.A., A comparison of subgrid-scale models for large-eddy simulations of convection in the Earth's core, *Geophys. J. Int.*, 2003, vol. 153, pp. 753–765.

Busse, F.H., Thermal instabilities in rapidly rotating systems, *J. Fluid Mech.*, 1970, vol. 44, pp. 441–460.

Christensen, U. and Aubert, J., Scaling properties of convection-driven dynamos in rotating spherical shells and application to planetary magnetic fields, *Geophys. J. Int.*, 2006, vol. 166, pp. 97–114.

Frick, P.G., *Turbulentnost': podkhody i modeli* (Turbulence: Approaches and Models), 2nd ed., Moscow–Izhevsk: Regulyarnaya Khaoticheskaya Mekhanika, 2010.

Glatzmaier, G.A. and Roberts, P.H., A three-dimensional convective dynamo solution with rotating and finitely conducting inner core and mantle, *Phys. Earth Planet. Inter.*, 1995, vol. 91, pp. 63–75.

Glatzmaier, G.A. and Roberts, P.H., An anelastic evolutionary geodynamo simulation driven by compositional and thermal convection, *Phys. D (Amsterdam, Neth.)*, 1996, vol. 97, pp. 81–94.

Hejda, P. and Reshetnyak, M., Effects of anisotropy in the geostrophic turbulence, *Phys. Earth Planet. Inter.*, 2009, vol. 177, pp. 152–160.

Jones, C.A., Boronski, P., Brun, A.S., Glatzmaier, G.A., Gastine, T., Miesch, M.S., and Wicht, J., Anelastic convec-

tion-driven dynamo benchmarks, *Icarus*, 2011, vol. 216, pp. 120–135.

Jones, C.A., Convection-driven geodynamo models, *Phil. Trans. R. Soc. London*, 2000, vol. A358, pp. 873–897.

Jones, C.A., Thermal and compositional convection in the outer ñîrå, in *Treatise on Geophysics. Core Dynamics,* Schubert, G., Ed., Amsterdam: Elsevier, 2007, vol. 8, pp. 131–185.

Krause, F. and Rädler, K.-H., *Mean Field Magnetohydrodynamics and Dynamo Theory*, Berlin: Akademie-Verlag, 1980.

Lesieur, M., *Turbulence in Fluids,* Netherlands: Kluwer Academic Publisher, 1990.

Matsushima, M., A scale-similarity model for the subgrid-scale flux with application to MHD turbulence in the Earth's core, *Phys. Earth Planet. Inter.*, 2005, vol. 153, pp. 74–82.

Pedlosky, J., *Geophysical Fluid Dynamics*, New York: Springer, 1987.

Reshetnyak, M. and Hejda, P., Direct and inverse cascades in the geodynamo, *Nonlin. Proc. Geophys.*, 2008, vol. 15, pp. 873–880.

Reshetnyak, M. and Hejda, P., Kinetic energy cascades in the quasi-geostrophic convection in the spherical shell, *Phys. Scr.*, 2012, vol. 86, pp. 018408–018412.

Rudiger, G. and Hollerbach, R., *The Magnetic Universe: Geophysical and Astrophysical Dynamo Theory*, Weinheim: Wiley-VCH, 2004.

Schrinner, M., Schmitt, D., Cameron, R., and Hoyng, P., Saturation and time dependence of geodynamo models, *Geophys. J. Int.*, 2010, vol. 182, pp. 675–681.

Shimkanin, J., Hejda, P., and *Saxonbergova-Jankovichova*, *D.*, Convection in rotating non-uniformly stratified spherical fluid shells in dependence on Ekman and Prandtl numbers, *Phys. Earth Planet. Inter.*, 2010, vol. 178, pp. 39–47.

Shimkanin, J., Hejda, P., and Saxonbergova, D., Hydromagnetic dynamos in rotating non-uniformly stratified spherical fluid shells in dependence on the Rayleigh number, *Phys. Earth Planet. Inter.*, 2011, vol. 3, pp. 100–106.

Translated by M. Nazarenko